Optica Applicata, Vol. XLVI, No. 1, 2016
DOI: 10.5277/oa160102

Evolution properties of multi-Gaussian Schell model beams propagating in uniaxial crystal orthogonal to the optical axis

XINGYUAN LU, YAN SHEN, XINLEI ZHU, CHENGLIANG ZHAO*, YANGJIAN CAI

College of Physics, Optoelectronics and Energy and Collaborative Innovation Center of Suzhou Nano Science and Technology, Soochow University, Suzhou 215006, China

*Corresponding author: zhaochengliang@suda.edu.cn

An analytical formula for the multi-Gaussian Schell model is derived for the beam propagating in a uniaxial crystal orthogonal to the optical axis. The propagation properties of multi-Gaussian Schell model beams in a uniaxial crystal orthogonal to the optical axis is investigated by using the analytical formula. Some results are illustrated by numerical examples related to the propagation properties of multi-Gaussian Schell model beams. It is found that the propagation properties of the multi-Gaussian Schell model beams are very different from the propagation properties in the free space. They are closely related to the initial coherence and the ratio of the extraordinary and ordinary refractive indices. The results provide a way for studying the propagation properties of the multi-Gaussian Schell model beams in the uniaxial crystal orthogonal to the optical axis.

Keywords: propagation properties, partially coherent, uniaxial crystal.

1. Introduction

In recent years, the optical beams with flat intensity, called flat-topped beams, attracted much attention because of their wide applications in free-space optical communications, inertial confinement fusion, material thermal processing, nonlinear optics and electron acceleration [1–8]. At the same time, the super-Gaussian beam, flattened Gaussian beam, flat-topped beam and flat-topped multi-Gaussian beam have been used as theoretical models to describe the flat-topped beam [9–12]. The propagation properties of various flat-topped beams in different optical systems, such as free-space, paraxial optical system and turbulent atmosphere have been studied in detail [1, 4, 9–20]. The flat-topped beams were extended to the partially coherent case due to wide application of the partially coherent beams. BORGHI and SANTARSIERO studied the model decomposition of partially coherent flat-topped beams [21]. YAN ZHANG *et al.* investigated the spectrum properties of a partially coherent flat-topped beam in dispersive and gain media [22]. ALAVINEJAD studied the intensity and spectral properties of partially coherent flat-topped beams in turbulent atmosphere [23, 24]. BAYKAL and EYYUBOĞLU studied the scintillations of an incoherent flat-topped Gaussian beam in turbulence [25].

Due to wide application in various fields of the flatted-topped beam, there are many methods which can be used to generate the flatted-topped beam. In 1999, XU GUANG HUANG *et al.* used a flat-top beam shaper which was fabricated by laser-assisted chemical etching to obtain the flat-top beam [26]. In 2003, MILER *et al.* introduced a method of using the holographic Gaussian gratings to transform the Gaussian beams into super-Gaussian beams of the fourth degree [27]. In 2007, TARALLO *et al.* tested the Fabry–Pérot resonator to achieve the flat top beam shape [28]. In 2009, LITVIN and FORBES used two resonator systems of intra-cavity for generating flat-top-like beams [29]. The spatial light modulator was also used to generate the flat-top beam by HAOTONG MA *et al.* in 2010 [30]. More recently, FEI WANG and YANGJIAN CAI reported the experimental generation of a partially coherent flat-topped beam [31]. SAHIN and KOROTKOVA introduced a beam model named the multi-Gaussian Schell model (MGSM) beam [32]; it can generate the flat beams at far field through propagating in free space and in some linear random media [33]. Furthermore JI CANG *et al.* introduced the propagation properties of the MGSM beams passing through the atmospheric turbulence [34].

On the other hand, in 1990 SIEGMAN introduced the propagation factor (also known as M^2-factor) which is a particularly important property of an optical laser beam, and is regarded as a beam quality factor in many practical applications [35]. In 1991, GORI *et al.* extended the definition of M^2-factor from the coherent beam to the partially coherent beam [36]. Since then, the M^2-factor of the partially coherent beam has been widely studied [37–39]. The results show that the M^2-factor of a partially coherent beam depends on its beam profile and initial spatial coherence. Therefore, we can control the M^2-factor of a partially coherent beam by choosing a suitable beam profile and initial spatial coherence. In this paper, we investigate the behavior of the MGSM sources during the propagation through a uniaxial crystal orthogonal to the optical axis. Based on the Huygens–Fresnel integral and the Winger distribution function (WDF), the analytical expression for the spectral density, the degree of coherence, the propagation factor, the effective radius of curvature and the Rayleigh range of MGSM beams in uniaxial crystals are derived.

2. Theory

The geometry of the propagation of a laser beam in a uniaxial crystal orthogonal to the optical axis is shown in Fig. 1. We assume that a MGSM beam, which is polarized in the x-direction, is incident on a uniaxial crystal at the plane $z = 0$. The optical axis of the crystal coincides with the x-axis, and the dielectric tensor of the crystal can be expressed as

$$\varepsilon = \begin{bmatrix} n_e^2 & 0 & 0 \\ 0 & n_o^2 & 0 \\ 0 & 0 & n_o^2 \end{bmatrix} \tag{1}$$

where n_o and n_e are the ordinary and extraordinary refractive indices, respectively.

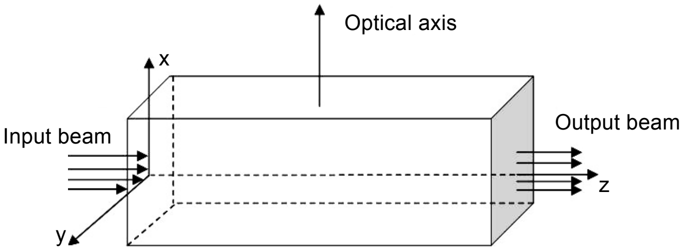

Fig. 1. Geometry of the MGSM beam propagates in a uniaxial crystal orthogonal to the optical axis x.

The most general form for any Schell-type cross-spectral density (CSD) of a random field at the planar source surface is

$$W^{(0)}(\mathbf{r}_1, \mathbf{r}_2; w) = \sqrt{S^{(0)}(\mathbf{r}_1; w)}\sqrt{S^{(0)}(\mathbf{r}_2; w)}\,\mu^{(0)}(\mathbf{r}_1 - \mathbf{r}_2; w) \tag{2}$$

$$S^{(0)}(\mathbf{r}, w) = \exp\left(-\frac{\mathbf{r}^2}{2\sigma^2}\right) \tag{3}$$

$$\mu^{(0)}(\mathbf{r}_1 - \mathbf{r}_2; w) = \frac{1}{C_0}\sum_{m=1}^{M}\binom{M}{m}\frac{(-1)^{m-1}}{m}\exp\left(-\frac{|\mathbf{r}_2 - \mathbf{r}_1|^2}{2m\delta^2}\right) \tag{4}$$

where $\mathbf{r}_1$ and $\mathbf{r}_2$ are two-dimensional position vectors, w is the angular frequency, $S^{(0)}$ is the spectral density, σ is the rms width of the source, and $\mu^{(0)}$ is the spectral degree of coherence of the source, $C_0 = \sum_{m=1}^{M}\frac{(-1)^{m-1}}{m}\binom{M}{m}$ is the normalization factor, $\binom{M}{m}$ stand for binomial coefficients, and δ is the rms correlation width. One can get the CSD by using the Eqs. (2)–(4) as follows:

$$W_x^{(0)}(\mathbf{r}_1, \mathbf{r}_2; w) = \exp\left(-\frac{\mathbf{r}_1^2 + \mathbf{r}_2^2}{4\sigma^2}\right)\frac{1}{C_0}\sum_{m=1}^{M}\binom{M}{m}\frac{(-1)^{m-1}}{m}\exp\left(-\frac{|\mathbf{r}_2 - \mathbf{r}_1|^2}{2m\delta^2}\right) \tag{5}$$

In this paper, we consider the MGSM beam propagating through a uniaxial crystal orthogonal to the optical axis. Within the framework of paraxial propagation, the relationship between the input and output transverse electric fields in the uniaxial crystal are as follows:

$$E_x(\rho_x, \rho_y, z) = \frac{kn_o}{2i\pi z}\exp(ikn_e z)\iint E_x(x, y, 0) \times$$
$$\times \exp\left\{-\frac{k}{2izn_e}\left[n_o^2(\rho_x - x)^2 + n_e^2(\rho_y - y)^2\right]\right\}\mathrm{d}x\mathrm{d}y \tag{6}$$

$$E_y(\rho_x, \rho_y, z) = \frac{kn_o}{2i\pi z}\exp(ikn_o z)\iint E_y(x, y, 0) \times \times \exp\left\{-\frac{kn_o}{2iz}\left[(\rho_x - x)^2 + (\rho_y - y)^2\right]\right\}\mathrm{d}x\mathrm{d}y \tag{7}$$

$$\mathbf{W}(\rho_{x_1}, \rho_{y_1}, \rho_{x_2}, \rho_{y_2}, z) = \langle E^*_\alpha(\rho_{x_1}, \rho_{y_1}, z)E_\beta(\rho_{x_2}, \rho_{y_2}, z)\rangle \tag{8}$$

Substituting Eq. (5) into Eqs. (6)–(8), one can obtain

$$W_x(\boldsymbol{\rho}_1, \boldsymbol{\rho}_2, z) = \frac{k^2 n_o^2}{4\pi^2 z^2}\iiiint W_x^{(0)}(\mathbf{r}_1, \mathbf{r}_2, 0) \times \times \exp\left\{-\frac{k}{2izn_e}\left[n_o^2(\rho_{x_1} - x_1)^2 + n_e^2(\rho_{y_1} - y_1)^2\right]\right\} \times \times \exp\left\{-\frac{k}{2izn_e}\left[n_o^2(\rho_{x_2} - x_2)^2 + n_e^2(\rho_{y_2} - y_2)^2\right]\right\}\mathrm{d}\mathbf{r}_1\mathrm{d}\mathbf{r}_2 \tag{9}$$

After the integral we get the CSD of the MGSM in the uniaxial crystal.

$$W_x(\boldsymbol{\rho}, z) = \frac{1}{C_0}\sum_{m=1}^{M}\binom{M}{m}\frac{(-1)^{m-1}}{m}\frac{k^2 n_o^2}{4z^2\sqrt{\left(a_3 a_4 - \frac{1}{4\delta_m^4}\right)\left(a_1 a_2 - \frac{1}{4\delta_m^4}\right)}} \times \times \exp\left\{\frac{k^2 n_o^2 \delta_m^2(1 - \delta_m^2 a_1 - \delta_m^2 a_2)}{z^2 n_e^2(4a_1 a_2 \delta_m^4 - 1)}\rho_x^2 + \frac{k^2 n_e^2 \delta_m^2(1 - \delta_m^2 a_3 - \delta_m^2 a_4)}{z^2(4a_3 a_4 \delta_m^4 - 1)}\rho_y^2\right\} \tag{10}$$

The m-th term in the sum (5) can be evaluated in the same manner, we treat $\sqrt{m}\,\delta$ as δ_m, $\delta_m = \sqrt{m}\,\delta$, and with $\rho_{x_1} = \rho_{x_2} = \rho_x$, and $\rho_{y_1} = \rho_{y_2} = \rho_y$,

$$a_1 = 1/4\sigma^2 + 1/2\delta_m^2 + kn_o^2/2izn_e \tag{11a}$$

$$a_2 = 1/4\sigma^2 + 1/2\delta_m^2 - kn_o^2/2izn_e \tag{11b}$$

$$a_3 = 1/4\sigma^2 + 1/2\delta_m^2 + kn_e/2iz \tag{11c}$$

$$a_4 = 1/4\sigma^2 + 1/2\delta_m^2 - kn_e/2iz \tag{11d}$$

3. Evolution properties of MGSM beams in a uniaxial crystal

In this section, the evolution properties of multi-Gaussian Schell model beams propagating in a uniaxial crystal orthogonal to the optical axis are studied based on the cross-spectral density formulae derived above.

Figure 2 shows the contours and the corresponding cross-line of a MGSM beam propagating in free space at several propagation distances and several values of index M. The other parameters are $k = 2\pi/\lambda$, $\sigma = 10$ mm, $\delta = 1$ mm, $\lambda = 632$ nm and $z_R = 2\pi\sigma^2/\lambda$. One can find that in free space the intensity distribution of the MGSM keeps the Gaussian distribution at a small propagation distance from Fig. 2. When the prop-

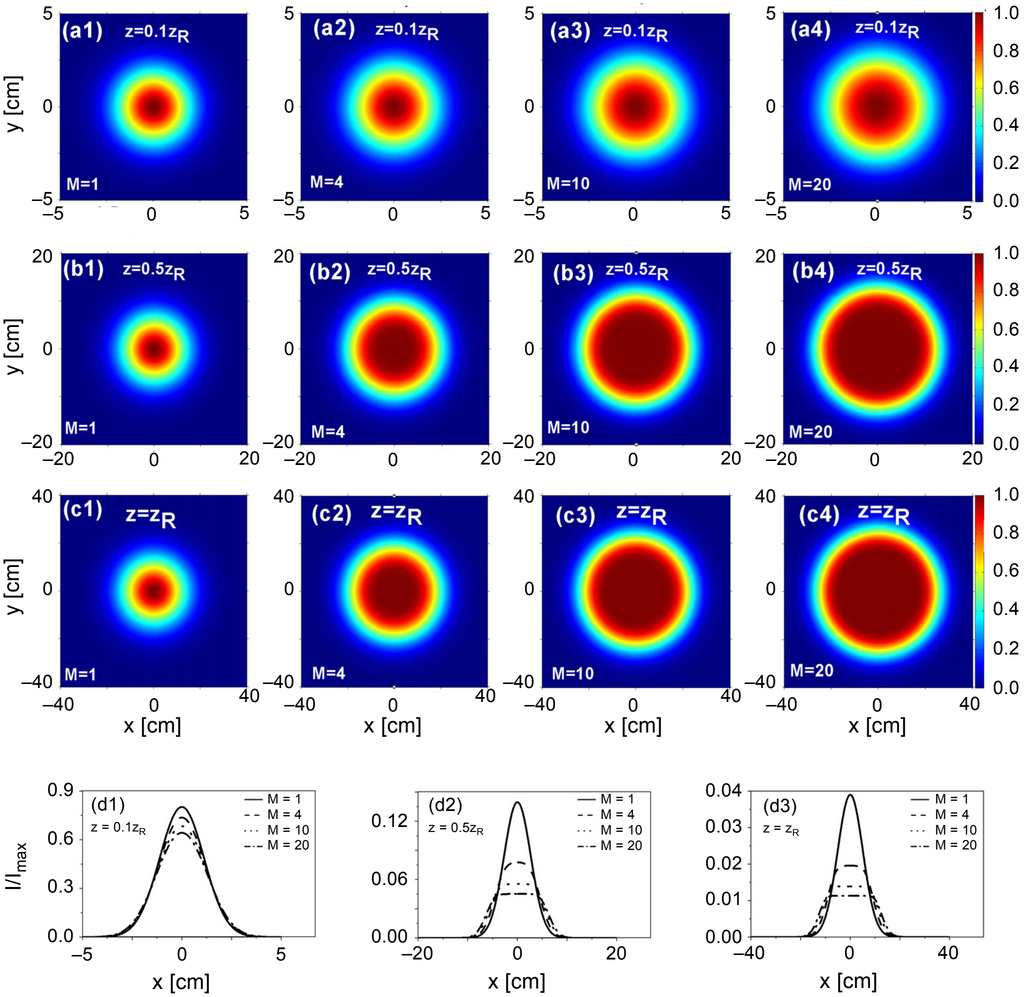

Fig. 2. The intensity distribution of a MGSM beam in free space at several propagation distances z and several values of the index M.

agation distance increases, the intensity distribution becomes flat-topped, and the beam spot becomes flatter with the increase in the index M.

For the convenience of comparison, the corresponding results of the MGSM in uniaxial crystals are shown in Fig. 3. Figure 3 shows the CSD of the MGSM beam at the ratio of $n_e/n_o = 1.5$ in uniaxial crystals. One finds that in the near fields the CSD are similar to those in free space, but these properties become increasingly obvious as the propagation distance increases due to the anisotropic affection of the crystals. When the MGSM beams pass through the crystal, the beam spot of a MGSM beam

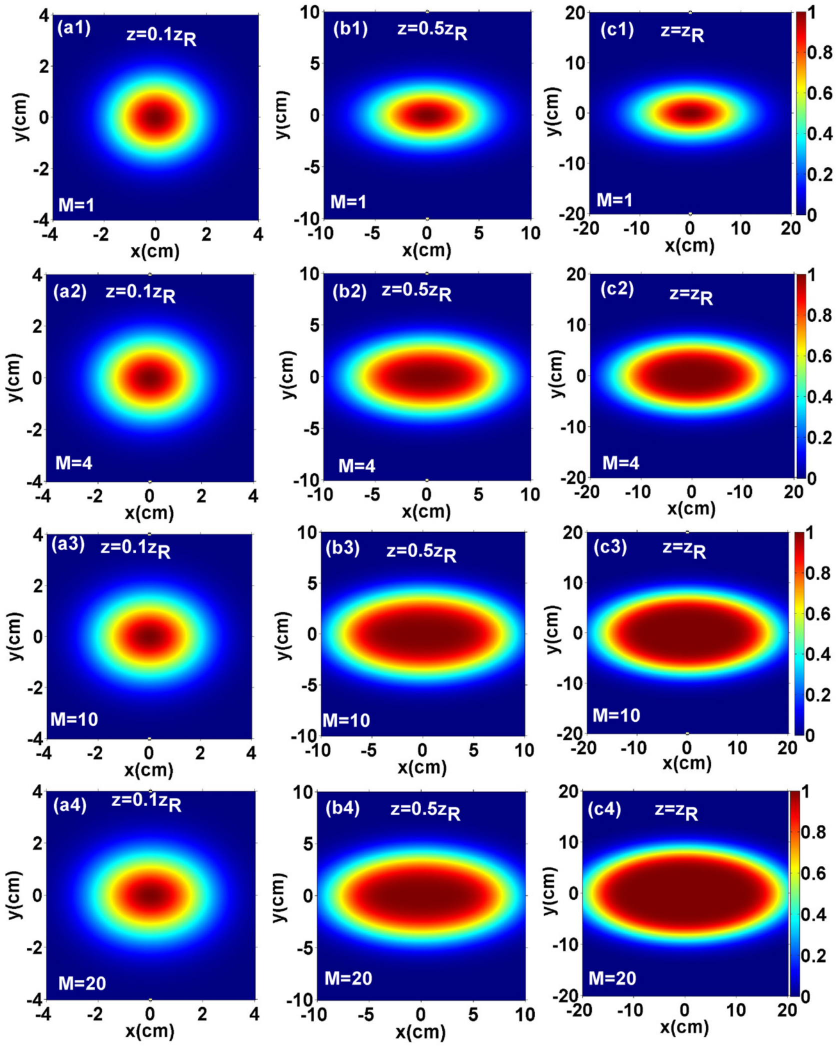

Fig. 3. The intensity distribution of a MGSM beam in a uniaxial crystal with $n_e/n_o = 1.5$ at several propagation distances z and several values of the index M.

becomes a quasi-elliptical Gaussian beam. Furthermore as the value of M increases, the spot becomes more elliptical. Therefore, one can get the elliptically flat-topped beam at far fields.

The normalized intensity contour graph of a MGSM beam in uniaxial crystals orthogonal to the optical axis at $z = z_R$ for different ratios of n_e/n_o and M is shown in Fig. 4. It is clear that the ratio of n_e/n_o affects the far field intensity distribution strongly. The beam spots in y-direction of the MGSM become more elliptical as increases the value of M and decreases the ratio n_e/n_o with $n_e/n_o < 1$. At the same time, the beam spots in x-direction of the MGSM become more elliptical as increases the value of M and the ratio n_e/n_o with $n_e/n_o > 1$. Therefore, from Figs. 3 and 4, one can get that the uniaxial crystals can affect the propagation properties of the MGSM beams passing

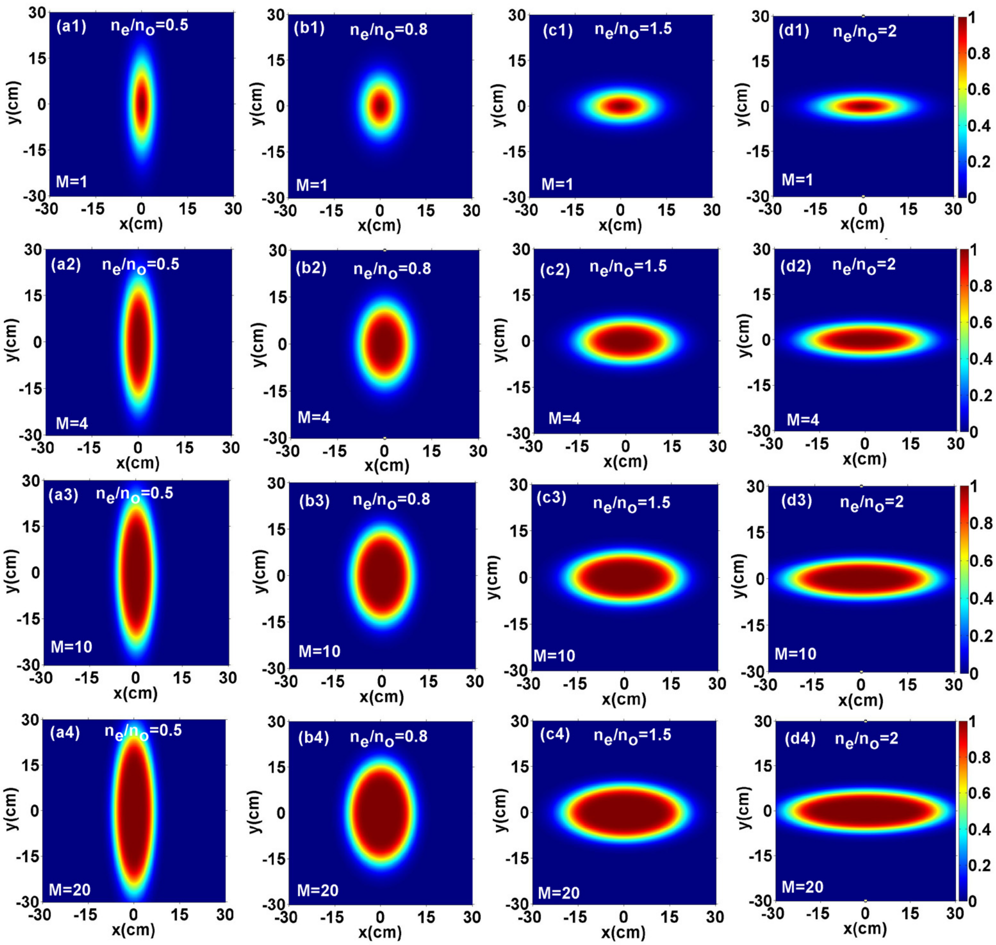

Fig. 4. The distribution of a MGSM beam in a uniaxial crystal at the propagation distance $z = z_R$, for different values of the uniaxial crystal parameters n_e/n_o and the index M.

through them. Therefore, one can modulate the intensity distribution of the MGSM beams by using different ratios of n_e/n_o of uniaxial crystals.

The degree of coherence of the MGSM beam at a pair of transverse points is defined by the formulae [40]. The spectral degree of coherence is directly related to the source's parameters, if we set $\boldsymbol{\rho} = 2\boldsymbol{\rho}_1 = -2\boldsymbol{\rho}_2$ then we can get the formula of the degree of coherence

$$\mu(\boldsymbol{\rho}, z, w) = \frac{W(\boldsymbol{\rho}_1, \boldsymbol{\rho}_2, z; w)}{S(0, z; w)} = \\ = \Upsilon\left[\sum_{m=1}^{M}\binom{M}{m}\frac{(-1)^{m-1}}{m}\frac{k^2 n_o^2}{4z^2\sqrt{\left(a_3 a_4 - \frac{1}{4\delta_m^4}\right)\left(a_1 a_2 - \frac{1}{4\delta_m^4}\right)}}\right]^{-1} \tag{12}$$

where

$$\Upsilon = \sum_{m=1}^{M}\binom{M}{m}\frac{(-1)^{m-1}}{m}\frac{k^2 n_o^2}{4z^2\sqrt{\left(a_3 a_4 - \frac{1}{4\delta_m^4}\right)\left(a_1 a_2 - \frac{1}{4\delta_m^4}\right)}} \times \\ \times \exp\left\{-\frac{k^2 n_o^2 \delta_m^2(1 + \delta_m^2 a_1 + \delta_m^2 a_2)}{z^2 n_e^2(4a_1 a_2 \delta_m^4 - 1)}\frac{\rho_x^2}{4} - \frac{k^2 n_e^2 \delta_m^2(1 + \delta_m^2 a_3 + \delta_m^2 a_4)}{z^2(4a_3 a_4 \delta_m^4 - 1)}\frac{\rho_y^2}{4}\right\} \tag{13}$$

Figure 5 explores the behavior of μ of the MGSM passing through a uniaxial crystals. One can find that at near fields, the profiles of μ resemble those in the source plane which can be found in [32]. With increasing propagation distance, the shape of curve becomes Gaussian-like (Figs. 5**d**–5**i**), and the dependence on M gradually disappears. Moreover, one can observe that the value of coherence width increases with increasing the value of n_e/n_o.

Within the validity of the paraxial approximation, the WDF of the MGSM beams in a uniaxial crystal can be expressed in terms of the CSD by the formula [41, 42]

$$h(\boldsymbol{\rho}, \boldsymbol{\theta}, z) = \left(\frac{k}{2\pi}\right)^2 \int_{-\infty}^{\infty}\int_{-\infty}^{\infty} W_x(\rho_x, \rho_y, q_x, q_y; z)\exp(-ik\theta_x q_x - ik\theta_y q_y)\mathrm{d}q_x \mathrm{d}q_y \tag{14}$$

where $\boldsymbol{\theta} = (\theta_x, \theta_y)$ denotes the angle between the vector of interest and the z-direction, $k\theta_x$ and $k\theta_y$ are the wave vector components along the x- and y-axis, respectively.

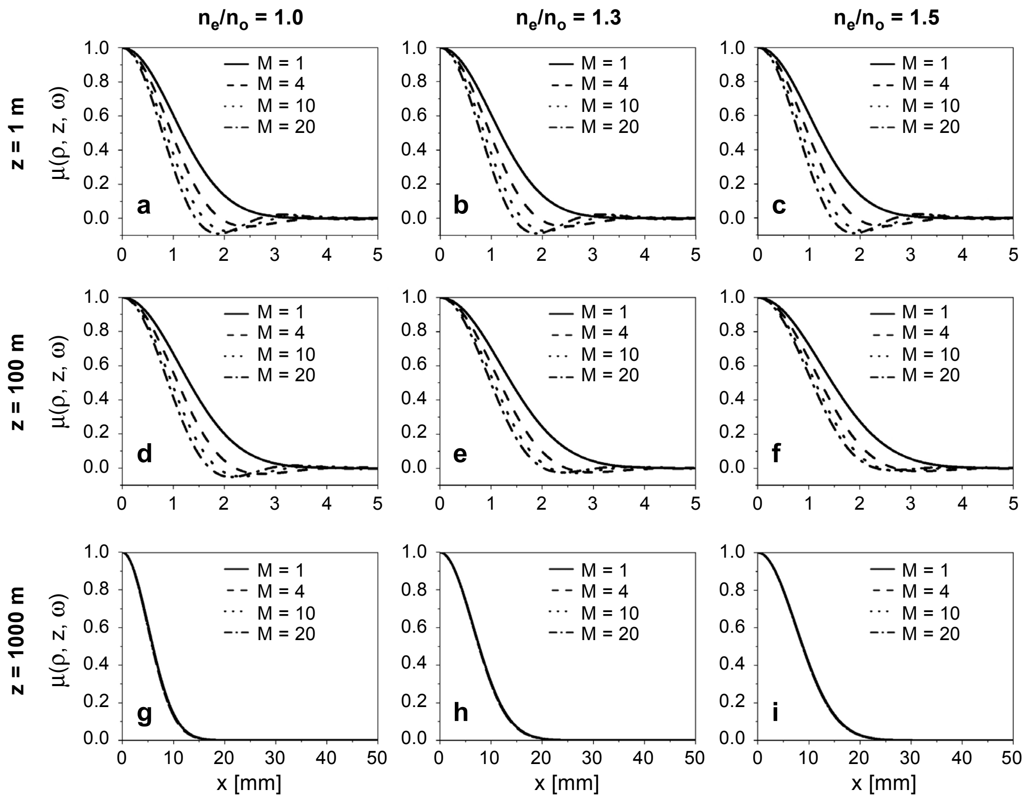

Fig. 5. The behavior of μ of the MGSM passing through a uniaxial crystal as a function of transverse difference variable $|\boldsymbol{\rho}|$ for several values of z and the ratio of n_e/n_o.

In this paper we set $\rho_{x_1} = \rho_x + q_x/2$, $\rho_{y_1} = \rho_y + q_y/2$, $\rho_{x_2} = \rho_x - q_x/2$, $\rho_{y_2} = \rho_y - q_y/2$. Substituting Eq. (10) into Eq. (14), one can obtain (after tedious integration) the expression

$$h(\boldsymbol{\rho}, \boldsymbol{\theta}, z) = \frac{1}{C_0}\sum_{m=1}^{M}\binom{M}{m}\frac{(-1)^{m-1}}{m}\frac{k^2}{\pi\left(\dfrac{1}{2\sigma^2} + \dfrac{2}{\delta_m^2}\right)} \times \\ \times \exp\left\{-\frac{1}{2\sigma^2}\left[\left(\rho_x - \frac{zn_e}{n_o^2}\theta_x\right)^2 + \left(\rho_y - \frac{z}{n_e}\theta_y\right)^2\right]\right\}\exp\left[-\frac{k^2(\theta_x^2 + \theta_y^2)}{\dfrac{1}{2\sigma^2} + \dfrac{2}{\delta_m^2}}\right] \tag{15}$$

Based on the second-order moments of the WDF [43–46], one can get the second -order moments of the MGSM beams which propagate in the uniaxial crystal as follows:

$$Q = \int_{-\infty}^{\infty}\int_{-\infty}^{\infty}\int_{-\infty}^{\infty}\int_{-\infty}^{\infty} h(\boldsymbol{\rho}, \boldsymbol{\theta}, z)\mathrm{d}^2\rho\,\mathrm{d}^2\theta = 2\pi\frac{1}{C_0}\sum_{m=1}^{M}\binom{M}{m}\frac{(-1)^{m-1}}{m}\sigma^2 \tag{16}$$

$$\langle\rho_x^2(z)\rangle = \frac{1}{Q}\int_{-\infty}^{\infty}\int_{-\infty}^{\infty}\int_{-\infty}^{\infty}\int_{-\infty}^{\infty}\rho_x^2 h(\rho_x, \rho_y, \theta_x, \theta_y, z)\mathrm{d}\rho_x\mathrm{d}\rho_y\mathrm{d}\theta_x\mathrm{d}\theta_y = \\ = \frac{1}{C_0}\sum_{m=1}^{M}\binom{M}{m}\frac{(-1)^{m-1}}{m}\frac{\sigma^2\pi(4\sigma^2+\delta_m^2)\left(\dfrac{z^2n_e^2}{2\sigma^2n_o^4}+\dfrac{2k^2\sigma^2\delta_m^2}{4\sigma^2+\delta_m^2}\right)}{Qk^2\delta_m^2} \tag{17}$$

$$\langle\rho_y^2(z)\rangle = \frac{1}{Q}\int_{-\infty}^{\infty}\int_{-\infty}^{\infty}\int_{-\infty}^{\infty}\int_{-\infty}^{\infty}\rho_y^2 h(\rho_x, \rho_y, \theta_x, \theta_y, z)\mathrm{d}\rho_x\mathrm{d}\rho_y\mathrm{d}\theta_x\mathrm{d}\theta_y = \\ = \frac{1}{C_0}\sum_{m=1}^{M}\binom{M}{m}\frac{(-1)^{m-1}}{m}\frac{\sigma^2\pi(4\sigma^2+\delta_m^2)\left(\dfrac{z^2}{2\sigma^2n_e^2}+\dfrac{2k^2\sigma^2\delta_m^2}{4\sigma^2+\delta_m^2}\right)}{Qk^2\delta_m^2} \tag{18}$$

$$\langle\theta_x^2(z)\rangle = \frac{1}{2}\frac{\partial^2\langle\rho_x^2(z)\rangle}{\partial z^2} = \frac{1}{C_0}\sum_{m=1}^{M}\binom{M}{m}\frac{(-1)^{m-1}}{m}\frac{\pi(4\sigma^2+\delta_m^2)n_e^2}{2Qk^2\delta_m^2n_o^4} \tag{19}$$

$$\langle\theta_y^2(z)\rangle = \frac{1}{2}\frac{\partial^2\langle\rho_y^2(z)\rangle}{\partial z^2} = \frac{1}{C_0}\sum_{m=1}^{M}\binom{M}{m}\frac{(-1)^{m-1}}{m}\frac{\pi(4\sigma^2+\delta_m^2)}{2Qk^2\delta_m^2n_e^2} \tag{20}$$

$$\rho_x(z)\theta_x(z)\rangle = \frac{1}{2}\frac{\partial\langle\rho_x^2(z)\rangle}{\partial z} = \\ = \frac{1}{C_0}\sum_{m=1}^{M}\binom{M}{m}\frac{(-1)^{m-1}}{m}\frac{\pi z}{2Qk^2}\left(\frac{n_e}{n_o^2}\right)^2\left(1+\frac{4\sigma^2}{\delta_m^2}\right) \tag{21}$$

$$\langle\rho_y(z)\theta_y(z)\rangle = \frac{1}{2}\frac{\partial\langle\rho_y^2(z)\rangle}{\partial z} = \\ = \frac{1}{C_0}\sum_{m=1}^{M}\binom{M}{m}\frac{(-1)^{m-1}}{m}\frac{\pi z}{2Qk^2}\frac{1}{n_e^2}\left(1+\frac{4\sigma^2}{\delta_m^2}\right) \tag{22}$$

$$\langle \rho^2(z) \rangle = \langle \rho_x^2(z) \rangle + \langle \rho_y^2(z) \rangle =$$

$$= \frac{1}{C_0} \sum_{m=1}^{M} \binom{M}{m} \frac{(-1)^{m-1}}{m} \left[\frac{z^2 \pi (n_o^4 + n_e^4)(4\sigma^2/\delta_m^2 + 1)}{2Qk^2 n_e^2 n_o^4} + \frac{4\pi k^2 \sigma^4}{Qk^2} \right] \tag{23}$$

$$\langle \theta^2(z) \rangle = \langle \theta_x^2(z) \rangle + \langle \theta_y^2(z) \rangle =$$

$$= \frac{1}{C_0} \sum_{m=1}^{M} \binom{M}{m} \frac{(-1)^{m-1}}{m} \frac{\pi (n_o^4 + n_e^4)(4\sigma^2/\delta_m^2 + 1)}{2Qk^2 n_e^2 n_o^4} \tag{24}$$

$$\langle \rho(z)\theta(z) \rangle = \langle \rho_x(z)\theta_x(z) \rangle + \langle \rho_y(z)\theta_y(z) \rangle =$$

$$= \frac{1}{C_0} \sum_{m=1}^{M} \binom{M}{m} \frac{(-1)^{m-1}}{m} \frac{z\pi (n_o^4 + n_e^4)(4\sigma^2/\delta_m^2 + 1)}{2Qk^2 n_e^2 n_o^4} \tag{25}$$

The M^2-factor of a MGSM beam in a uniaxial crystal can be defined as follows [47–49]. After a tedious operation we can get

$$M^2(z) = kn_o(\langle \rho^2(z) \rangle \langle \theta^2(z) \rangle - \langle \rho(z)\theta(z) \rangle^2)^{1/2} =$$

$$= \frac{1}{C_0} \sum_{m=1}^{M} \binom{M}{m} \frac{(-1)^{m-1}}{m} \left[\frac{2\pi^2 \sigma^4 (n_o^4 + n_e^4)(4\sigma^2/\delta_m^2 + 1)}{Q^2 k^2 n_e^2 n_o^2} \right]^{1/2} \tag{26}$$

Figure 6 shows the M^2-factor distribution of a MGSM beam in a uniaxial crystal at several values of the uniaxial crystal parameters n_e/n_o and the index of M. In Fig. 6,

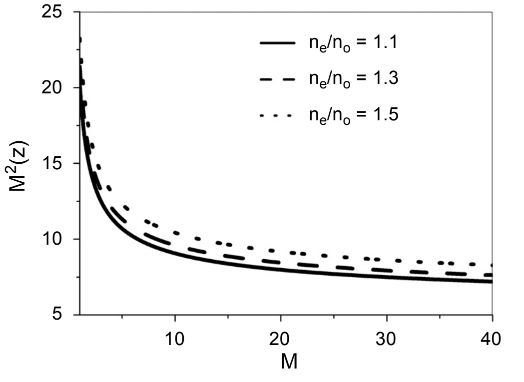

Fig. 6. M^2-factor distribution of a MGSM beam propagating in a uniaxial crystal with $z = 0.1z_R$ with different n_e/n_o and M.

one can see that the M^2-factor distribution of a MGSM beam in a uniaxial crystal decreases with an increase in the beam order M, while it increases with an increase of the ratio n_e/n_o.

Under the condition of $n_e = n_o = 1$ and $M = 1$, Eq. (26) can be reduced to

$$M^2(z) = (4\sigma^2/\delta^2 + 1)^{1/2} \tag{27}$$

Equation (27) shows that M^2-factor is independent of the propagation distance z; this result is in agreement with the conclusion derived for the case of a scalar GSM beam [49].

The Rayleigh range is an important beam parameter for characterizing the distance within which the laser beam can be considered effectively non-spreading. The Rayleigh range is defined as the distance z_R along the propagation direction of a beam from the beam waist to the place where the area of the cross-section is doubled [46, 50]. The range of the minimum effective radius of curvature is defined as the distance z_m along the propagation direction of a beam from the beam waist to the place where the effective radius of curvature (ERC) of the beam takes the minimum value,

$$\langle\rho^2(z_R)\rangle - 2\langle\rho^2(0)\rangle = 0 \tag{28}$$

$$\left.\frac{\mathrm{d}R(z)}{\mathrm{d}z}\right|_{z = z_m} = 0 \tag{29}$$

Substituting Eq. (23) into Eqs. (28) and (29), we can get the Rayleigh range of the MGSM beams in a uniaxial crystal as

$$z_R = z_m = 2k\sigma^2 n_e n_o^2\left[\sum_{m=1}^{M}\binom{M}{m}\frac{(-1)^{m-1}}{m}\frac{2}{(n_o^4 + n_e^4)(4\sigma^2/\delta_m^2 + 1)}\right]^{1/2} \tag{30}$$

We can find that the Rayleigh range z_R equals the range of the minimum effective radius of curvature z_m.

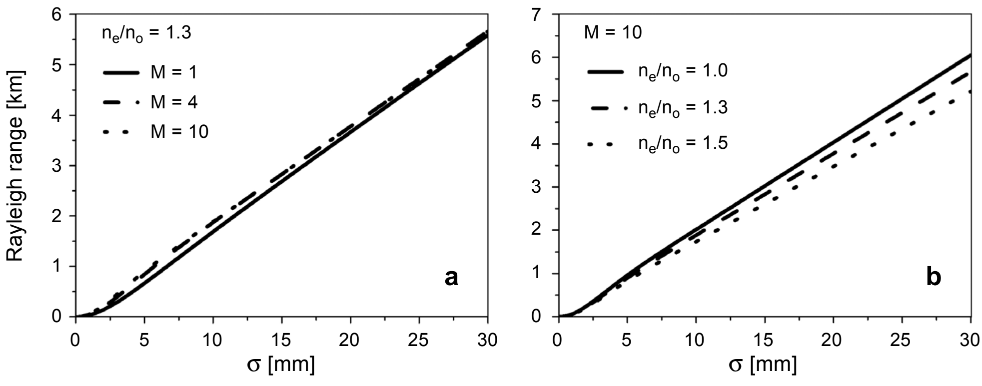

Fig. 7. Rayleigh range of a MGSM beam in uniaxial crystal for different values of σ.

Figure 7 illustrates the Rayleigh range of a MGSM beam in uniaxial crystals for different initial coherence width σ. From Fig. 7**a**, one can conclude that with an increase in the initial coherence width σ and the beam order M, the Rayleigh range also increases. The initial parameters of the uniaxial crystal such as ratio of n_e/n_o also can affect the Rayleigh range greatly, as we can see from Fig. 7**b** the Rayleigh range decreases with an increase of n_e/n_o.

According to [46, 50], the effective radius of curvature (ERC) of a MGSM beam at z can be defined in terms of the ratio of $\langle \rho^2 \rangle$ to $\langle \rho\theta \rangle$. It is clear that the effective radius of curvature defined by

$$R(z) = \frac{\langle \rho^2 \rangle}{\langle \rho(z)\theta(z) \rangle} = \sum_{m=1}^{M} \binom{M}{m} \frac{(-1)^{m-1}}{m} \left(z + \frac{8 n_o^4 n_e^2 k^2 \sigma^4}{z(n_o^4 + n_e^4)(4\sigma^2/\delta_m^2 + 1)} \right) \tag{31}$$

obeys the propagation equation as does the wave front curvature of an ideal Gaussian beam.

Figure 8 shows the ERC of a MGSM beam in uniaxial crystal *versus* the propagation distance z for different values of n_e/n_o and M. One finds from Fig. 8 that with increasing of the ratio of n_e/n_o, the ERC decreases, and it increases with the value of M.

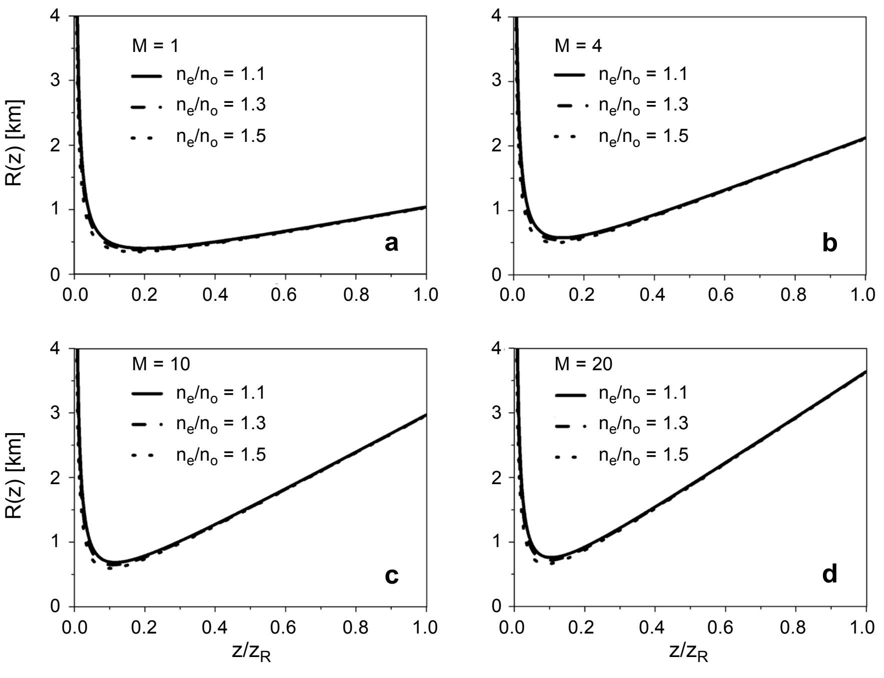

Fig. 8. ERC of a MGSM beam in uniaxial crystal *versus* the propagation distance z for different values of n_e/n_o.

It is the fact that the initial parameters of the uniaxial crystal and the beam order *M* affect the ERC greatly.

4. Conclusion

We have investigated the evolution properties a MGSM beam in a uniaxial crystal with help of the extended Huygens–Fresnel integral and the WDF. We have derived the analytic formulas for the CSD, the degree of coherence, the propagation factor, the Rayleigh range, and the ERC of the MGSM in uniaxial crystals. From the results one can find that the ratio of n_e/n_o and the index M have great influence on the propagation properties. The results show that one can modulate the intensity distribution of a MGSM beam by changing the parameters of the uniaxial crystal. It will be useful in some applications, such as optical trapping and nonlinear optics.

Acknowledgements – This research is supported by the National Natural Science Foundation of China under Grant Nos. 11274005, 11374222, the Project Funded by the Priority Academic Program Development of Jiangsu Higher Education Institutions, and the Universities Project Sponsored by the Scientific Research Foundation for the Returned Overseas Chinese Scholars, State Education Ministry, the Qing Lan Project of Jiangsu Province, the 2013 High Educational Reform Project of Soochow University under Grant No. 5731501713.

Reference

[1] COWAN D.C., RECOLONS J., ANDREWS L.C., YOUNG C.Y., *Propagation of flattened Gaussian beams in the atmosphere: a comparison of theory with a computer simulation model*, Proceedings of SPIE **6215**, 2006, article 62150B.

[2] EYYUBOĞLU H.T., ARPALI Ç., BAYKAL Y., *Flat topped beams and their characteristics in turbulent media*, Optics Express **14**(10), 2006, pp. 4196–4207.

[3] BAYKAL Y., EYYUBOĞLU H.T., *Scintillation index of flat-topped Gaussian beams*, Applied Optics **45**(16), 2006, pp. 3793–3797.

[4] YANGJIAN CAI, *Propagation of various flat-topped beams in a turbulent atmosphere*, Journal of Optics A: Pure and Applied Optics **8**(6), 2006, pp. 537–545.

[5] NISHI N., JITSUNO T., TSUBAKIMOTO K., MATSUOKA S., MIYANAGA N., NAKATSUKA M., *Two-dimensional multi-lens array with circular aperture spherical lens for flat-top irradiation of inertial confinement fusion target*, Optical Review **7**(3), 2000, pp. 216–220.

[6] COUTTS D.W., *Double-pass copper vapor laser master-oscillator power-amplifier systems: generation of flat-top focused beams for fiber coupling and percussion drilling*, IEEE Journal of Quantum Electronics **38**(9), 2002, pp. 1217–1224.

[7] LI WANG, JIANHUA XUE, *Efficiency comparison analysis of second harmonic generation on flattened Gaussian and Gaussian beams through a crystal $CsLiB_6O_{10}$*, Japanese Journal of Applied Physics, Part 1 **41**(12), 2002, pp. 7373–7376.

[8] WANG W., WANG P.X., HO Y.K., KONG Q., CHEN Z., GU Y., WANG S.J., *Field description and electron acceleration of focused flattened Gaussian laser beams*, Europhysics Letters **73**(2), 2006, pp. 211–217.

[9] BOWERS M.S., *Diffractive analysis of unstable optical resonator with super-Gaussian mirrors*, Optics Letters **17**(19), 1992, pp. 1319–1321.

[10] GORI F., *Flattened gaussian beams*, Optics Communications **107**(5–6), 1994, pp. 335–341.

[11] YAJUN LI, *Light beam with flat-topped profiles*, Optics Letters **27**(12), 2002, pp. 1007–1009.
[12] TOVAR A.A., *Propagation of flat-topped multi-Gaussian laser beams*, Journal of the Optical Society of America A **18**(8), 2001, pp. 1897–1904.
[13] AMARANDE S.-A., *Beam propagation factor and the kurtosis parameter of flattened Gaussian beams*, Optics Communications **129**(5–6), 1996, pp. 311–317.
[14] BORGHI R., SANTARSIERO M., VICALVI S., *Focal shift of focused flat-topped beams*, Optics Communications **154**(5–6), 1998, pp. 243–248.
[15] BAGINI V., BORGHI R., GORI F., PACILEO A.M., SANTARSIERO M., AMBROSINI D., SPAGNOLO G.S., *Propagation of axially symmetric flattened Gaussian beams*, Journal of the Optical Society of America A **13**(7), 1996, pp. 1385–1394.
[16] YANGJIAN CAI, QIANG LIN, *Properties of a flattened Gaussian beam in the fractional Fourier transform plane*, Journal of Optics A: Pure and Applied Optics **5**(3), 2003, pp. 272–275.
[17] XIAOLING JI, LU B., *Focal shift and focal switch of flattened Gaussian beams in passage through an aperture bifocal lens*, IEEE Journal of Quantum Electronics **39**(1), 2003, pp. 172–178.
[18] YANGJIAN CAI, QIANG LIN, *Light beams with elliptical flat-topped profiles*, Journal of Optics A: Pure and Applied Optics **6**(4), 2004, pp. 390–395.
[19] BORGHI R., *Elegant Laguerre–Gauss beams as a new tool for describing axisymmetric flattened Gaussian beams*, Journal of the Optical Society of America A **18**(7), 2001, pp. 1627–1633.
[20] YANGJIAN CAI, SAILING HE, *Partially coherent flattened Gaussian beam and its paraxial propagation properties*, Journal of the Optical Society of America A **23**(10), 2006, pp. 2623–2628.
[21] BORGHI R., SANTARSIERO M., *Modal decomposition of partially coherent flat-topped beams produced by multimode lasers*, Optics Letters **23**(5), 1998, pp. 313–315.
[22] YAN ZHANG, BIN ZHANG, QIAO WEN, *Changes in the spectrum of partially coherent flat-top light beam propagating in dispersive or gain media*, Optics Communications **266**(2), 2006, pp. 407–412.
[23] ALAVINEJAD M., GHAFARY B., *Turbulence-induced degradation properties of partially coherent flat-topped beams*, Optics and Lasers in Engineering **46**(5), 2008, pp. 357–362.
[24] ALAVINEJAD M., GHAFARY B., RAZZAGHI D., *Spectral changes of partially coherent flat topped beam in turbulent atmosphere*, Optics Communications **281**(8), 2008, pp. 2173–2178.
[25] BAYKAL Y., EYYUBOĞLU H.T., *Scintillations of incoherent flat-topped Gaussian source field in turbulence*, Applied Optics **46**(22), 2007, pp. 5044–5050.
[26] XU GUANG HUANG, WANG M.R., CHANGYUAN YU, *High-efficiency flat-top beam shaper fabricated by a nonlithographic technique*, Optical Engineering **38**(2), 1999, pp. 208–213.
[27] MILER M., AUBRECHT I., PALA J., *Holographic Gaussian to flat-top beam shaping*, Optical Engineering **42**(11), 2003, pp. 3114–3122.
[28] TARALLO M.G., MILLER J., AGRESTI J., D'AMBROSIO E., DESALVO R., FOREST D., LAGRANGE B., MACKOWSKY J.M., MICHEL C., MONTORIO J.L., MORGADO N., PINARD L., REMILLEUX A., SIMONI B., WILLEMS P., *Generation of a flat-top laser beam for gravitational wave detectors by means of a nonspherical Fabry–Perot resonator*, Applied Optics **46**(26), 2007, pp. 6648–6654.
[29] LITVIN I.A., FORBES A., *Intra-cavity flat-top beam generation*, Optics Express **17**(18), 2009, pp. 15891 –15903.
[30] HAOTONG MA, ZEJIN LIU, PU ZHOU, XIAOLIN WANG, YANXING MA, XIAOJUN XU, *Generation of flat-top beam with phase-only liquid crystal spatial light modulator*, Journal of Optics **12**(4), 2010, article 045704.
[31] FEI WANG, YANGJIAN CAI, *Experimental generation of a partially coherent flat-topped beam*, Optics Letters **33**(16), 2008, pp. 1795–1797.
[32] SAHIN S., KOROTKOVA O., *Light soureces generating far fields with tunable flat profiles*, Optics Letters **37**(14), 2012, pp. 2970–2972.
[33] KOROTKOVA O., SAHIN S., SHCHEPAKINA E., *Multi-Gaussian Schell-model beams*, Journal of the Optical Society of America A **29**(10), 2012, pp. 2159–2164.
[34] JI CANG, XU FANG, XU LIU, *Propagation properties of multi-Gaussian Schell-model beams through ABCD optical systems and in atmospheric turbulence*, Optics and Laser Technology **50**, 2013, pp. 65–70.

[35] SIEGMAN A.E., *New developments in laser resonators*, Proceedings of SPIE **1224**, 1990, pp. 2–14.
[36] GORI F., SANTARSIERO M., SONA A., *The change of width for a partially coherent beam on paraxial propagation*, Optics Communications **82**(3–4), 1991, pp. 197–203.
[37] XIAOLIANG CHU, BIN ZHANG, QIAO WEN, *Generalized M^2 factor of a partially coherent beam propagating through a circular hard-edged aperture*, Applied Optics **42**(21), 2003, pp. 4280–4284.
[38] SANTARSIERO M., GORI F., BORGHI R., CINCOTTI G., VAHIMAA P., *Spreading properties of beams radiated by partially coherent Schell-model sources*, Journal of the Optical Society of America A **16**(1), 1999, pp. 106–112.
[39] BIN ZHANG, XIAOLIANG CHU, QIANG LI, *Generalized beam-propagation factor of partially coherent beams propagating through hard-edged apertures*, Journal of the Optical Society of America A **19**(7), 2002, pp. 1370–1375.
[40] WOLF E., *Unified theory of coherence and polarization of random electromagnetic beams*, Physics Letters A **312**(5–6), 2003, pp. 263–267.
[41] BASTIAANS M.J., *Wigner distribution function and its application to first-order optics*, Journal of the Optical Society of America **69**(12), 1979, pp. 1710–1716.
[42] LIU D.J., ZHOU Z.X., *Wigner distribution function matrix of electromagnetic beams propagating through uniaxial crystals orthogonal to the optical axis*, The European Physical Journal D **58**(3), 2010, pp. 333–338.
[43] WEBER H., *Propagation of higher-order intensity moments in quadratic-index media*, Optical and Quantum Electronics **24**(9), 1992, pp. S1027–S1049.
[44] MARTÍNEZ-HERRERO R., MEJÍAS P.M., *Second-order spatial characterization of hard-edge diffracted beams*, Optics Letters **18**(19), 1993, pp. 1669–1671.
[45] MARTÍNEZ-HERRERO R., MEJÍAS P.M., ARIAS M., *Parametric characterization of coherent, lowest-order Gaussian beams propagation through hard-edge apertures*, Optics Letters **20**(2), 1995, pp. 124–126.
[46] FEI WANG, YANGJIAN CAI, *Second-order statistics of twisted Gaussian Schell-model beam in turbulent atmosphere*, Optics Express **18**(24), 2010, pp. 24661–24672.
[47] FRIBERG A.T., SUDOL R.J., *Propagation parameters of Gaussian Schell-model beams*, Optics Communications **41**(6), 1982, pp. 383–387.
[48] SHIJUN ZHU, YANGJIAN CAI, *M^2-factor of a stochastic electromagnetic beam in a Gaussian cavity*, Optics Express **18**(26), 2010, pp. 27567–27581.
[49] SHIJUN ZHU, YANGJIAN CAI, KOROTKOVA O., *Propagation factor of a stochastic electromagnetic Gaussian Schell-model beam*, Optics Express **18**(12), 2010, pp. 12587–12598.
[50] GBUR G., WOLF E., *The Rayleigh range of Gaussian Schell-model beams*, Journal of Modern Optics **48**(11), 2001, pp. 1735–1741.

Received July 8, 2015
in revised form September 25, 2015